Chemometric guided isolation of new triterpenoid saponins as acetylcholinesterase inhibitors from *Achyranthes bidentata* Blume

Shivani Puri,[a,b] Prithvi Pal Singh,[a,b] Prateek Singh Bora,[a,b] and Upendra Sharma [a,b,*]

[a] C-H Activation & Phytochemistry Lab, Chemical Technology Division CSIR-IHBT, Palampur, Himachal Pradesh, 176061, India.

[b] Academy of Scientific and Innovative Research (AcSIR), Ghaziabad-201002, India

***Correspondence:**

Dr. Upendra Sharma, C-H Activation & Phytochemistry Lab, Chemical Technology Division, CSIR-IHBT, Palampur, Himachal Pradesh-176061, India;

Email:upendraihbt@gmail.com; upendra@ihbt.res.in

Highlights

- Fifty-six compounds were tentatively identified in the extract and fractions of *A. Bidentata* seeds using UPLC-IM-Q-TOF-MS/MS analysis.
- Two new triterpenoid saponins along with three known compounds were purified from water fraction using chemometric guided approach.
- The extract, fractions and isolated saponins demonstrated encouraging potential for inhibiting acetylcholinesterase in *in vitro* and *in silico* studies.
- Chikusetsusaponin IVa [(**5**); IC_{50}: 63.72 µM] showed mixed type of AchE inhibition in the enzyme kinetic studies.

Abstract

Achyranthes bidentata Blume is an annual herb widely used as functional food and for ethnomedicinal purposes in Traditional Chinese medicine. Its seeds are widely used as cereal grain substitutes due to their excellent nutritional composition and health benefits. In current study, chemical profiling with chemometric guided approach was adopted for the tentative identification of fifty-six compounds based on UPLC-IM-Q-TOF-MS/MS analysis. Chemometric guided approach also led to the isolation of two previously undescribed triterpenoid saponins, named as, achyranosides A-B (**1**-**2**) along with three known compounds (**3**-**5**) from water fraction of *A. bidentata* seeds. The structure elucidation of isolated molecules was done by using NMR, HR-ESI-MS, FT-IR and GC-FID techniques. Chikusetsusaponin IVa (**5**) exhibited most promising inhibition (IC_{50} values of 63.72 µM) of acetylcholinesterase *in vitro* with mixed type of AChE inhibition in enzyme kinetic studies. Additionally, *in-silico* studies disclosed the underlying molecular interactions and binding free energy between ligands and the binding sites. The current study demonstrated the effectiveness of chemometric guided integrated approach for the phytochemical exploration and isolation of new oleanane-type triterpenoid saponins from *A. bidentata* seeds.

Keywords: *Achyranthes bidentata* Blume, Chemometric guided approach, Triterpenoid saponins, Acetylcholinesterase inhibitory activity, Enzyme kinetics, *In silico* studies.

1. Introduction

Achyranthes bidentata Blume (Amaranthaceae), commonly known as Puthkanda (Hindi), is an annual herb of the *Achyranthes* genus mainly found in India, China, Japan, and Korea. The roots and seeds of the plant are extensively used as functional foods and cereal grain substitutes due to their excellent nutritional composition and health benefits (Zhang, Zhang, Zhang, Wang, & Yan, 2018). It is an important dietary ingredient in various health foods such as tea, wines, soups and other medicated foods (Yi, Li, Wang, Wu, & Liu, 2022). *A. bidentata* seeds have 1.6-2.4 times higher levels of crude protein than conventional grains such as barley, rice, wheat, and corn. In addition, seeds also contain substantially higher amount of minerals and edible oil with lower saturated/unsaturated fat ratio (Marcone, Jahaniaval, Aliee, & Kakuda, 2003; Yi, Li, Wang, Wu, & Liu, 2022).

Besides its nutritional excellence, *A. bidentata* is a well-documented folk medicine in the world's oldest pharmacopeia "Shen nong Ben cao Jing" utilized for various ethnomedicinal purposes such as for the treatment of amenorrhea, lumbago, gonalgia, edema, epistaxis etc. Triterpenoid saponins, polysaccharides, polypeptides, and ketosteroids are the major class of phytochemicals reported from the roots of *A. bidentata* which possess neurotrophic, neuroprotective, antiosteoporosis, antitumor and immunomodulatory activities (He, Wang, Fang, Chang, Ning, Guo, et al., 2017).

So far, only eight different compounds has been isolated from the seeds of *A. bidentata* (Dong, Yan, Zheng, Huai, & Tan, 2010). However, despite its ubiquitous abundance and nutritional importance, the systematic scientific study to understand the phytochemical profile of its seeds is still lacking. Bioactivity-guided isolation is the classical tool for isolation of bioactive compounds from medicinal plants however it is time and resource intensive process which lead to repetitive isolation of known compounds.

Recently, chemometrics have been extensively applied in the field of natural product chemistry for the detection of bioactive compounds, chemotaxonomical identification, and quality control

purposes. Chemometric-guided isolation is an innovative approach to prioritize and accelerate the isolation of novel compounds from complex botanical mixtures (Sá, da Silva, & de CS Nunomura, 2022). It helps to extract relevant information on phytochemical profile, identify distinct patterns and characteristic features of interest and also aids in dereplication.

In continuation of our research interest in the discovery of new bioactive molecules from medicinal plants, herein, we have adopted the chemometric guided isolation approach to target the isolation of new compounds as well as to improve knowledge regarding chemical profile of the seeds of the plant. The chemometric analysis and chemical profiling of *A. bidentata* seeds extract and fractions has been carried out using UPLC-IM-Q-TOF-MS/MS analysis. Further, based on chemometric observations, isolation and characterization of the two previously undescribed oleanane-type triterpenoid saponins, named achyranosides A-B (**1, 2**) along with three known compounds, 3-O-[*β*-D-xylopyranosyl-(1→2)]-[*α*-L-rhamnopyranosyl-(1→3)]-*β*-D-glucuronopyranosyl-28-O-*β*-D-gluco-pyranside-3*β*-hydroxy-olean-12-en-28-oate (**3**), momordin IIc (**4**) and chikusetsusaponin IVa (**5**) has been done. Compounds (**3, 4**) have been isolated for the first time from *Achyranthes* genus. The oleanane-type triterpenoid saponins are known for their significant neuroprotection against neurodegenerative disorders where acetylcholinesterase enzyme is one of the main culprits causing imbalanced cholinergic neurotransmission. Thus, the isolated molecules were evaluated for their AChE inhibitory activity *in vitro.* Moreover, the mode of inhibition and binding interactions of the isolated compounds was also studied by the enzyme kinetics and *in silico* studies.

2. Material and methods

2.1. General experimental procedures and instruments

The chemometric analysis was done using Umetric SIMCA software version 17.0 (Umea,

Sweden). Chemical profiling and HR-ESI-MS was done on a high-resolution Agilent 6560 Ion Mobility Q-TOF LC/MS system (Agilent, Santa Clara, USA). Compounds were isolated by employing the column chromatography (CC) technique using silica gel (mesh size: 60-120 & 230-400), reverse phase C18 silica fully, and Diaion HP-20 resin. The structure elucidation was done via ^{1}H (600 MHz) and ^{13}C (150 MHz) NMR experiments performed on a Bruker Avance-600 MHz NMR spectrometer. FT-IR spectra and optical rotations were measured using Shimadzu IR Prestige-21spectrophotometer and Anton Parr Modular compact polarimeter 100 (MCP 100). Bio Tek Synergy H1 plate reader was used for bioactivity evaluation. The *in-silico* studies were performed using Maestro software Schrodinger Inc.

2.2. Chemicals and reagents

The CC and HPLC-grade, solvents were purchased from S. D. Fine-Chem Ltd and Merck India Pvt. Ltd. The silica gel (60-120, 230-400, and reverse phase C18 entirely end-capped) and Diaion HP-20 resin was acquired from Merck Life Science Private Limited. Formic acid, methanol-d_4, acetylcholinesterase from *electrophorus electricus*, acetylthiocholine iodide (ATCI), 5-thio-2-nitrobenzoic acid (DTNB), and galantamine were purchased from Sigma Aldrich. Molecular grade dimethyl sulfoxide (DMSO) was procured from HIMEDIA.

2.3. Plant material collection and extraction

The seeds of *A. bidentata* Blume (1.5 Kg) were collected from Palampur (altitude: 1200 m, Latitude: 32°6'39.1"N; Longitude: 76°32'10.51"E), Himachal Pradesh, India. Taxonomy experts authenticated the plant material, and the herbarium sample was submitted at the CSIR-IHBT, Palampur, H.P. India (Voucher no. PLP18306). The shade-dried and powdered seeds (1.5 Kg) of *A. bidentata* were percolated using *n*-hexane (3L) for 24 h. The defatted seed powder was percolated thrice using 2L ethanol: water (80: 20) for 24 h at room temperature. The obtained extracts were dried on a rotatory evaporator at 50 °C and lyophilized to obtain

40.3 g of *n*-hexane extract and 177.6 g of hydroethanolic extract (ABSPE). The subsequent fractionation of the hydroethanolic extract was performed using *n*-hexane, ethyl acetate, and *n*-butanol to obtain 0.5 g of *n*-hexane (ABSHF), 19.2 g of ethyl acetate (ABSEAF), 129.3 g of *n*-butanol (ABSBF) and 41.0 g of water (ABSWF) fractions. The samples for LC-MS analysis were prepared at a concentration of 10 mg/ml and filtered with 0.22 µm syringe filter. The samples were stored at 4˚C for further analysis.

2.4. UPLC-IM-Q-TOF-MS/MS-based chemometric analysis and chemical profiling

The chromatographic analysis of extracts and different fractions was performed using high-resolution Agilent 6560 UPLC-IM-Q-TOF LC/MS system equipped with Eclipse PlusC18 RRHD (2.1 mm x 150 mm, 1.8 µm). The binary gradient elution system was used for chromatographic separation. The mobile phase consisted of water (0.1% formic acid) as solvent A and acetonitrile (0.1% formic acid) as solvent B at a flow rate of 0.26 ml/min. The gradient elution method of 25 minutes time interval was as follows: 0-5 min 68% A, 5-11 min 50% A, 11-15 min 10% A, 15-17 min 10% A, 17-25 min 68% A. MS detection was done using electrospray ionization in both positive and negative ion mode with nitrogen gas at the flow rate of 12 L/min at 350 °C. Nebulizer was maintained at 30 psig with a nozzle voltage of 500 V. The preprocessing of raw data obtained from the UPLC-IM-Q-TOF LC/MS analysis was done using MZmine-2.53 software with different feature-finding methods (Pluskal, Castillo, Villar-Briones, & Orešič, 2010). The principal component analysis (PCA) was done using Umetric SIMCA version 17.0 (Umea, Sweden). Further, discriminating variables were identified using the loading and variable trend plots. The R^2 (goodness of fit) for the developed model was found to be 0.98. The MS/MS data was processed by Agilent MassHunter Qualitative analysis B.07.00 software. The compound identification was carried out by comparing mass spectra and their fragmentation patterns with the literature, METLIN secondary metabolite database, and dictionary of natural product database.

2.5. Isolation and characterization of compounds

The column chromatography (CC) of water fraction (40 g) was performed using Diaion HP-20 resin with water: methanol (100:0-0:100) solvent system. Five fractions of 500 ml each (WFA-WFE) were collected, dried, and lyophilized. The subfraction WFD (1.5 g) was subjected to reverse phase C18 silica gel CC using water: methanol (100:0 - 0:100) solvent system, and 12 fractions (WFD_A-WED_L) were collected. The CC of WED_I afforded compound **3** (33.0 mg) using methanol: water (40.60:60.40). Reverse phase CC of subfraction WFD_G (700 mg) done using water: methanol (100.0:0.100) led to the isolation of compound **1** (15 mg) and compound **2** (11 mg). Further, reverse phase CC of fraction WFD_J (10.6 g) was also performed using water: methanol (100.0:0.100) to give compounds **4** (15 mg) and **5** (9 mg).

2.5.1. Acid hydrolysis and gas chromatography analysis

To determine the absolute configuration of sugars, 3 mg of each compound (**1** and **2**) were hydrolyzed with 20 ml of 1 M HCl in 1,4-dioxane/H_2O (1:1) at 80 °C for 6 h under nitrogen atmosphere. The reaction mixture was neutralized by passing through neutral ion exchange free base resin Amberlyst A21. Then, the mixture was partitioned with water and chloroform. The identification of the aqueous layer was primarily done on TLC by comparison with standard sugars using ternary mobile phase [chloroform: methanol: water (8:5:1)]. The derivatization of hydrolyzed as well as standard sugars was done by treating with pyridine and N, O-Bis (trimethylsilyl) trifluoroacetamide containing 1% trimethylchlorosilane (1:1) at room temperature for 12 h and followed by GC-FID analysis. The GC parameters were as follows: carrier gas: Helium; ion source temperature 200 °C and ionization energy: 70 eV; temperature program- injector temperature: 240 °C; column temperature: initial temp. 70 °C & hold for 4 min, then increased to 280 °C at 12 °C/min & then hold for 10 min.

2.5.2. Analysis of sugars

The retention time (rt) of derivatized standard sugars was found at 19.80 min (D-glucuronic acid), 17.00 min (D-xylose), 16.05 min (L-rhamnose), and 18.73 min (D-glucose) (Fig. S32-S35). The monosaccharides in compound **1** were identified at rt 19.89 min (D-glucuronic acid), 18.50 min (D-glucose) and 16.91 min (D-xylose) (Fig. S36). Similarly, for compound **2**, monosaccharides were observed at rt 19.66 min (D-glucuronic acid), 18.59 min (D-glucose), and 16.91 min (D-xylose) (Fig. S37).

2.6. Evaluation of biological activity

2.6.1. In vitro acetylcholinesterase inhibitory activity

The acetylcholinesterase enzyme inhibitory activity of the extract/ fractions and isolated compounds was evaluated using Ellman's method with slight modifications (Ellman, Courtney, Andres Jr, & Featherstone, 1961). Acetylthiocholine iodide was used as the substrate to study the inhibition of the acetylcholinesterase enzyme obtained from electric eel. Initially, 150 µl of 0.1 M potassium phosphate buffer of pH 8.0, 10 µl of test samples dissolved in buffer (50-200 µM), and 20 µl of enzyme (0.1 U/ml) were added in triplicates in a 96 well plate and incubated for 15 min at 25°C. Subsequently, 10 µl of 10 mM 5-thio-2-nitrobenzoic acid (DTNB) solution and 10 µl of 14 mM ATCI solution was added to the wells to initiate the enzymatic reaction. The enzymatic hydrolysis of acetylthiocholine into thiocholine can be determined by the formation of yellow colored chromophore developed as a product of reaction between thiocholine and Ellman reagent (DTNB). After incubation for 10 mins, the optical density of the 96 well plate was measured at 412 nm using a microplate reader. Galantamine hydrobromide was used as a positive control. The percent inhibition of AChE was determined using the formula A-S/A*100, where A is the optical density without a test sample & S is the optical density with a test sample. The IC_{50} value of isolated compounds was determined graphically using GraphPad Prism 9.0 software and was reported as mean ± SD.

2.6.2. Enzyme kinetics

The kinetic studies of AChE inhibition by the isolated compounds (**1-5**) were performed using a similar protocol mentioned above. The different inhibitor concentration (50-200 µM) was used for the kinetic experiments at varying substrate concentrations, i.e., 43.75-1400 µM. The type of inhibition and *Ki* values for each inhibitor were determined using Lineweaver-Burk plot and a secondary plot. The results of the kinetic experiments were analyzed using GraphPad software 9.0.

2.7. In-silico studies

The molecular docking studies were performed using Maestro software (Schrodinger Inc.). The crystal structure of AChE (PDB ID:1C2O) with 4.20 Å resolution was downloaded from RCSB Protein Data Bank. The protein's preprocessing, optimization, and minimization of crystal structure were performed via the protein preparation wizard. The chemical structures of the isolated compounds and galantamine were imported from ChemBioDraw Ultra 14.0. The compounds were prepared using Ligprep tool to generate energy-minimized molecular structures. The site mapping tool and receptor grid generation module were employed to generate an effective binding pocket. Finally, the binding affinities of isolated compounds with the binding site were estimated using the Glide module under extra precision mode.

3. Results and discussion

3.1. Chemometric analysis and chemical profiling

The analysis of mass spectra of extract and fractions in both the ionization mode displayed multiple base peaks ranging from *m/z* 100-1600. The observed characteristic mass ions belonging to different class of specialized metabolites clearly indicated the complexity of extracts and fractions. Hence, the preprocessed UPLC-IM-Q-TOF-MS/MS data was

statistically modelled to identify chemical differences among the extract and fractions. Specifically, principal component analysis (PCA) detects clusters or outliers in the data set and helps to identify chemical differences among different samples (Bora, Agrawal, Kaushik, Puri, Sahal, & Sharma, 2023). PCA score plot of *A. bidentata* seeds extract and fractions revealed that the sample clustered into distinct classes based upon different mass ions present in them. The ethyl acetate fraction was found to be distinct compared to the water and *n*-butanol fractions in the score plots which indicated chemical differences between them (Fig. 1A) whereas the proximity of water and butanol fraction indicated their chemical similarity. The complementary nature of the loadings and score plot helps to determine the variables responsible for the distinction of samples in the score plot (Anokwuru, Sandasi, Chen, van Vuuren, Elisha, Combrinck, et al., 2021). Hence, analysis of the loading plots (Fig. 1B) and the variable trend plot (Fig. 1C) along with reported literature revealed the presence of characteristic mass ions (m/z 955, 941, 939, 823, 793, 455, 439 etc.,) belonging to the class of triterpenoid saponins in the water and *n*-butanol fraction (Li, Wei, Qi, Chen, Ren, & Li, 2010). The ethyl acetate fraction displayed mass ions (*m/z* 314, 342, 623, 641 etc.,) belonging to the class of phenolic acids and ecdysteroids (Ying-Ying, Jia-Yuan, Chang-Liang, Zhang, Yang, Shuai, et al., 2022) (Cao, Gu, Zhao, Tang, Cui, Shi, et al., 2017). Further, these corresponding mass ions were identified in positive and negative ionization mode based on mass spectral data comparison with reported literature. A total of fifty-six compounds including triterpenoid saponins, phenolic acids, ecdysteroids, flavonoid glycosides, coumarins and oligosaccharide were identified in the extract and fractions of *A. bidentata* seeds (Table 1).

Triterpenoid saponins: A total of thirty-six triterpenoid saponins were identified in *A. bidentata* extract and fractions. The identification of triterpenoid saponins was done based on the appearance of characteristic oleanane moiety mass fragment and sugar residues (such as glucose, rhamnose, glucuronic acid, and xylose) in the structure. The peak 17 identified at rt

9.369 min has shown a deprotonated molecular ion peak at *m/z* 1101.42 $[M-H]^-$ in negative ionization mode. Its fragment ions peaks at *m/z* 955.34 $[M-H-Rha]^-$, and 569.16 $[M-H-Rha-2Glu-H_2O-COO]^-$ (Fig. 2A) were obtained by sequential loss of one rhamnose and two glucose units and were identified as 3-O-[*β*-D-glucopyranosyl-(1→2)-*α*-L-rhamnopyranosyl-(1→3)-*β*-D-glucuronopyranosyl]-28-O-*β*-D-glucopyranosyl oleanolic acid (Cao, et al., 2017). The peak 22 at rt 9.828 min exhibited a protonated molecular ion peak at *m/z* 957.50 $[M+H]^+$ in positive ionization mode with major fragment ions at *m/z* 795.45 $[M+H-Glu]^+$, 632.39 $[M-2Glu]^+$, and 456.35 $[M-2Glu-Glucu]^+$ (Fig. 2B) was annotated as ginsenoside Ro/chikusetsusaponin V (Li, Wei, Qi, Chen, Ren, & Li, 2010). Similarly, the peak 35 at rt 12.125 min showed a deprotonated molecular ion peak at *m/z* 1117.50 $[M-H]^-$ with fragment ions at *m/z* 955.34 $[M-H-C_5H_6O_6]^-$ and 793.33 $[M-H-C_5H_6O_6-Glu]$, which is consistent with the structure of Achyranthoside D (Li, Wei, Qi, Chen, Ren, & Li, 2010). Furthermore, the peak 47 at rt 17.106 min showing ion peak at *m/z* 939.38 $[M-H]^-$ along with fragment ions at *m/z* 777.34 $[M-H-Glu]^-$, 597.21 $[M-H-Glu-Xyl-H_2O-HCHO]^-$, and 579.24 $[M-H-Glu-Xyl-HCHO-2H_2O]^-$ was assigned as pseudoginsenoside Rt1 methyl ester (Mi, Xu, Hong, Jiang, Chen, Li, et al., 2023). The other triterpenoid saponins were also identified in the same manner.

Phenolic acids: Four phenolic acids were identified based on characteristic C_6-C_3 phenylpropanoid skeleton in positive and negative ionization modes. The peak 14 at rt 7.581 showed a protonated molecular ion peak at *m/z* 314.14 $[M+H]^+$. The peak at m/z 336.12 $(M+Na)^+$ and its fragment at m/z 177.05 $[M+H-C_8H_{10}O-CH_3]^+$ obtained by the loss of 4-hydroxyphenyl ethyl and methyl group was annotated as N-trans-feruloyltramine (Cao, et al., 2017). Similarly, the peak 15 at rt 8.077 min showed deprotonated molecular ion peak at *m/z* 342.07 $[M-H]^-$ and its mass fragments at *m/z* 327.15 $[M-H-CH_3]^-$, and 178.93 $[M-H-C_9H_{10}NO_2]^-$ were obtained by the loss of a methyl and [2-(4-hydroxy-3-methoxyphenyl) ethyl]) group. This was identified as *N-trans*-feruloyl-3-methoxytyramine (Fig. 2C) (Cao, et al., 2017).

Ecdysteroids: Six ecdysteroids were also identified in the extract and fractions of *A. bidentata* seeds. The peak 2 at rt 1.774 min showed protonated molecular ion peak at *m/z* 481.31 $[M+H]^+$ and fragment ions at *m/z* 463.30 $[M+H-H_2O]^+$ and 445.29 $[M+H-2H_2O]^+$, was identified as 20-hydroxyecdysone (Fig. 2D) (Rostandy & Gao, 2019). Furthermore, the peak 4 at rt 2.194 have shown an intense adduct ion peak at *m/z* 525.22 $[M+HCOO]^-$ and deprotonated molecular ion peak at *m/z* 479.02 $[M-H]^-$. The elimination of characteristic cyclopentanoperhydrophenanthrene moiety leads to production of fragment ion at m/z 159.02 $[M-H-C_{19}H_{28}O_4]^-$ and was identified as 25S-Inokosterone (Ying-Ying, et al., 2022).

Other classes: Some flavonoid glycosides, coumarins, steroid saponins, and oligosaccharides were also identified based on a comparison of their molecular ion peak and fragmentation pattern with reported data in the literature (Table 1).

According to the contribution plot (Fig. 1D), the ions at m/z 421, 579, 823, 1087, 1101, 925, 955, 939, and 925 were responsible for the distinction of water fraction from average data set of the model. The mass spectrum of ion at m/z 1101.40 $(M-H)^-$ showed fragments at 925 $(M-H-Glucu)^-$, 779 $(M-H-Glucu-Rha)^-$, 647 $(M-H-Glucu-Rha-Xyl)^-$, and 485 $(M-H-Glucu-Rha-Xyl-Glu)^-$ which cannot be assigned to any known triterpenoid saponin as per literature reports. Similarly, 1087, 939, 955 mass ions and their fragments were annotated as unknown compounds as indicated by their mass fragments shown in Table 1. These compounds were determined to be an oleanane-type triterpenoid saponins based on their characteristic mass fragment of oleanolic acid aglycone moiety and glycone units. Hence, considering LC-MS and chemometric observations, the water fraction of *A. bidentata* seeds was further targeted for the isolation of new triterpenoid saponins.

3.2. Characterization of isolated compounds

The compound **1** was isolated as off-white amorphous powder with molecular formula $C_{47}H_{72}O_{20}$ calculated from its sodium adduct ion peak at *m/z* 979.4504 $[M+Na]^+$ (cal. for $C_{47}H_{72}O_{20}Na^+$ as 979.4509) in the HR-ESI-MS spectra (Fig. S9). The ^1H spectrum of compound **1** (Fig. S2) has shown six tertiary methyl signals [δ_H 0.79 (s), 0.91 (s), 0.93 (s), 0.97 (s), 1.14 (s), and 1.16 (s)], along with an olefinic proton signal [δ_H 5.25 (1H, t, J = 3.6)] and one oxygenated methine proton signal [δ_H 4.05 (1H, dd, J = 12.6, 4.8)] corresponding to the aglycon skeleton. Similarly, the ^{13}C NMR spectrum (Fig. S3) along with DEPT-135 (Fig. S4) and HSQC spectra (Fig. S5) revealed the presence of ten quaternary, six methyl groups, twelve methylene and nineteen methine carbons (including one olefinic carbon at δ_C 123.5 and fifteen oxygenated methine carbons) (Table 1). The observed characteristic signals indicated the presence of an olean-12-ene-type skeleton of the aglycone unit (Yuan, Wang, Zhang, Su, & Li, 2013). The oxygenated proton at δ_H 4.05 (H-3) showed major HMBC correlations (Fig. 3B, S6) with δ_C 181.4 (C-23)/ 12.2 (C-24)/ 105.3 (C-1′). Similarly, the HMBC correlation of methyl signal at δ_H 1.14 (Me-24) with δ_C 181.4 (C-23), and an upfield shift of C-24 (δ_C 12.2) indicated the presence of carboxylic group at C-23 position. The angular methyl signal at δ_H 0.97 (Me-25) showed HMBC correlation (Fig. S6) with δ_C 39.6 (C-1)/ 52.9 (C-5)/ 49.1(C-9) and 37.4 (C-10). The remaining methyl signals at δ_H 0.79 (Me-26) and 1.16 (Me-27) were assigned based on their HMBC correlations with δ_C 40.9 (C-8)/ 49.1 (C-9)/ 42.9 (C-14) and δ_C 40.9 (C-8)/ 42.9 (C-14)/ 28.8 (C-15), respectively. The neighboring methyl protons at δ_H 0.91 (Me-29) and 0.93 (Me-30) were assigned based on common HMBC correlation with δ_C 47.2 (C-19)/ 31.5 (C-20), and 34.8 (C-22).

The relative configuration of aglycone moiety was assigned based on α-orientation of H-3. The observed NOESY correlation (Fig. S8) between H-3/H-1′, H-3/H-2a indicated their presence on the same side and were assigned as α-oriented. The absence of a cross peak between H-3/Me-24 indicated the β-orientation of the methyl group (Me -24). Similarly, the NOESY

correlation between Me-24/ Me-25 and Me-25/Me-26 suggested their *β*-orientation. The *α*-orientation of Me-27 was assigned based on the absence of correlation between Me-26/Me-27 in the NOESY spectra of compound **1**. Based on these NOESY correlations, the ring fusions were determined as *trans* at A/B and C/D ring junctions. Hence, the aglycone moiety was assigned as 3*β*-hydroxy-olean-12-en-23-oic acid-28-oate.

The three anomeric protons were observed at δ_H 4.38 (d, J = 7.8), δ_H 4.52 (d, J = 7.2), and δ_H 5.38 (d, J = 8.4) corresponding to carbons at δ_C 105.3, δ_C 105.7, and δ_C 95.7, respectively. The downfield shift at C-3 (δ_C 86.4) and upfield shift at C-28 (δ_C 178.1) along with HMBC correlation (Fig. S6) of anomeric proton at δ_H 4.38 (GlcA-H-1′) with δ_C 86.4 (C-3) and δ_H 5.38 (Glc-H-1‴) with δ_C 178.1 indicated the glycosylation at C-3 and C-28. Similarly, the sugar linkage of anomeric proton at δ_H 4.52 (Xyl-H-1″) was established by its HMBC correlation with δ_C 86.1 (GlcA-C-3′). Hence compound **1** was determined as a 3,28-bidesmosidic saponin. The larger coupling constant (J >7 Hz) of anomeric protons of three sugars confirmed the *β*-configuration. The novelty of compound **1** resides in the COOH group at C-23 in combination with the defined sugars linkage pattern. The absolute configuration of sugars in compound **1** was determined by acid hydrolysis followed by derivatization and GC-FID analysis. The monosaccharides were determined as D-glucuronopyranosyl, D-xylopyranosyl, and D-glucopyranosyl. From NMR (1D and 2D), HR-ESI-MS, FT-IR, and GC-FID analysis compound **1** was assigned as 3-*O*-[*β*-D-xylopyranosyl-(1→3)]-*β*-D-glucuronopyranosyl-28-*O*-*β*-D-glucopyranside-3*β*-hydroxy-olean-12-en-23-oic-acid-28-oate and named as achyranoside A (Fig. 3A, B).

Compound **2** was isolated as off-white amorphous powder with the molecular formula $C_{47}H_{72}O_{19}$ calculated from its observed sodium adduct ion peak at *m/z* 963.4760 $[M+Na]^+$ (cal. for $C_{47}H_{72}O_{19}Na^+$ as 963.4560 $[M+Na]^+$) in the HR-ESI-MS spectra (Fig. S18). The

comparison of NMR data of compound **2** with compound **1** (Table 1) indicated the presence of a similar aglycone moiety along with 3,28-bidesmosidic saponin skeleton. The major distinction was observed at C-23 position of aglycone moiety. The presence of an additional methine proton at δ_H 9.39 (H-23) and its corresponding deshielded carbon at δ_C 208.9 (C-23) indicated the presence of an aldehyde group. The HMBC correlations (Fig. S15) of aldehydic proton at δ_H 9.38 (H-23) with neighboring carbon at δ_C 48.9 (C-5)/ δ_C 10.4 (C-24) and an upfield shift in the value of C-24 (δ_C 10.4) confirmed the presence of an aldehyde group at C-23 position. The relative stereochemistry and sugars linkages of compound **2** were established and found to be the same as compound **1** (Fig. S14-S17). The structure of compound **2** was established as 3-O-[*β*-D-xylopyranosyl-(1→3)]-*β*-D-glucuronopyranosyl-28-O-*β*-D-glucopyranside-3*β*-hydroxy-olean-12-en-23-al-28-oate and named as Achyranoside B (Fig. 3A, B).

The other three known compounds were characterized as 3-O-[*β*-D-xylopyranosyl-(1→2)]-[*α*-L-rhamnopyranosyl-(1→3)]-*β*-D-glucuronopyranosyl-28-O-*β*-D-gluco-pyranside-3*β*-hydroxy-olean-12-en-28-oate (**3**)(Kinjo, Suyama, & Nohara, 1995), momordin IIc (**4**) (Mizui, Kasai, Ohtani, & Tanaka, 1990) and chikusetsusaponin IVa (**5**) (Li, Wei, Qi, Chen, Ren, & Li, 2010) based on comparison with literature reports (Fig. 3A).

Achyranoside A (**1**): Off-white amorphous powder; $[\alpha]^{25}_D$ = -16.0° (CH_3OH; c = 0.5); Melting point: 215-217 °C; FT-IR (ZnSe) ν_{max} (cm^{-1}): 3414, 2900, 2322, 2013, 1724, 1404, 1045; HR-ESI-MS: *m/z* 979.4504 $[M+Na]^+$ (cal. for $C_{47}H_{72}O_{20}Na^+$). ^1H (600 MHz) and ^{13}C (150 MHz) NMR spectroscopic data see Table 1(Fig. S2-S10).

Achyranoside B (**2**): Off-white amorphous powder; $[\alpha]^{25}_D$ = -6.0° (CH_3OH; c = 0.5); Melting point: 186-188 °C; FT-IR (ZnSe) ν_{max} (cm^{-1}): 3649, 2966, 2337, 2025, 1720, 1072; HR-ESI-

MS: *m/z* 963.4760 $[M+Na]^+$ (cal. for $C_{47}H_{72}O_{19}Na^+$ as 963.4560 $[M+Na]^+$).^{1}H (600 MHz) and ^{13}C (150 MHz) NMR spectroscopic data see Table 1 (Fig. S11-S19).

3-O-[β-D-xylopyranosyl-(1→2)]-[α-L-rhamnopyranosyl-(1→3)]-β-D-glucuronopyranosyl-28-O-β-D-gluco-pyranside-3β-hydroxy-olean-12-en-28-oate (**3**): Pale white flakes; $[\alpha]^{25}_D$ = -22.0° (CH_3OH; c = 0.5); Melting point: 240-242 °C; FT-IR (ZnSe) ν_{max} (cm^{-1}): 3417, 2916, 2515, 2052, 1747, 1408, 1037; HR-ESI-MS: *m/z* 1095.5346 $[M+Na]^+$ (cal. for $C_{53}H_{84}O_{22}$ Na^+) (Fig. S20-S23) (Kinjo, Suyama, & Nohara, 1995).

Momordin IIc (**4**): Off white flakes; $[\alpha]^{25}_D$ = -8.0° (CH_3OH; c = 0.5); Melting point: 216-218 °C; FT-IR (ZnSe) ν_{max} (cm^{-1}): 3614, 2935, 2468, 2214, 1998, 1913, 1107; HR-ESI-MS: *m/z* 949.4745 $[M+Na]^+$ (cal. for $C_{47}H_{74}O_{18}$ Na^+) (Fig. S24-S27) (Mizui, Kasai, Ohtani, & Tanaka, 1990).

Chikusetsusaponin IVa (**5**): Light orange powder; $[\alpha]^{25}_D$ = -20.0 ° (CH_3OH; c = 0.5); Melting point: 217-219 °C; FT-IR (ZnSe) ν_{max} (cm^{-1}): 3456, 3302, 2924, 2468, 894; HR-ESI-MS: *m/z* 817.4330 $[M+Na]^+$ (cal. for $C_{42}H_{66}O_{14}Na^+$) (Fig. S28-S31) (Li, Wei, Qi, Chen, Ren, & Li, 2010).

3.3. In vitro acetylcholinesterase inhibitory activity and enzyme kinetics

The isolated triterpenoids saponins, extract/fractions were tested for their AChE inhibitory activity using Ellman's et al. method with slight modifications. The IC_{50} valuaes of isolated compounds, extract, and fractions are listed in Table S1**.** The IC_{50} values of compound **1** (75.6 µM) and **5** (63.7 µM) indicated potent AChE inhibitory activity, whereas the other three compounds (**2**-**4)** have shown moderate AChE enzyme inhibition (Fig. 4A). The presence of polar moieties, along with types and stereochemical configurations of functional groups, affect the triterpenoid saponins biological activity. Thus, the AChE inhibitory potential of seed extracts and isolated compounds might be due to multiple sugars at both C-3/28 positions of

aglycone moiety. This observation was further visualized by *in silico* studies. Additionally, the mechanism of AChE inhibition exhibited by the isolated compounds was investigated by enzyme kinetic study. The Michaelis-Menten equation was used to understand the relationship between reaction velocity and substrate concentration. The Lineweaver-Burk plot and the secondary plots (Fig. S38) of inhibitor concentration *vs* K_m apparent/V_{max} apparent (K_m app/V_{max} app) of the isolated compounds was developed to determine the type of inhibition and their inhibition constant (*Ki*). Isolated compounds exhibited mixed-type inhibition, as evident from increased Km and decreased V_{max} with increasing inhibitor concentration. The regression line of the Lineweaver-Burk plot does not intersect the X and Y-axes but it remains over or below the negative X-axis (Fig. 4B). Indicating both substrate and inhibitor can interact with enzyme simultaneously at two distinct sites, and their binding affinity gets affected by the interaction of other (Saboury, 2009). The lower K_i value (5-22 µM) of compounds (Table S1) were observed due to greater binding affinities between the inhibitor and the enzyme.

3.4. In silico studies

The binding affinities and interactions of the isolated compounds with the active site were visualized via molecular docking studies which disclosed that the standard drug (Galantamine) as well as isolated compounds occupied the same binding pocket on the surface of the protein (Fig. S46). The -OH groups and -COOH/-CHO group of compounds have shown H-bond interaction with multiple amino acids, which are part of the active and peripheral site of the AChE enzyme. The estimated binding energies of the compounds **1** (-13.14 kcal/mol) and **2** (-13.61 kcal/mol) were found to be the highest. The binding affinities of compounds **3** (-13.06 kcal/mol), **4** (-12.97 kcal/mol), and **5** (-9.91 kcal/mol) were also found to be good. Galantamine gave major H-bond interaction with active site residues such as Phe295, Tyr341, and Arg296.

Compound **1** showed five major H-bond interactions with active site (Fig. 4C) amino acid residues viz., Thr75, Leu76 of the active site gorge, Tyr341 residue of peripheral anionic site (PAS) and with Glu292, Val340 of surroundings of the active site of enzyme (Dvir, Silman, Harel, Rosenberry, & Sussman, 2010). Compound **2** also exhibited five H-bond interactions (Fig. 4C) as follows: Thr75, Leu76 of active site gorge, Trp286 residue of the anionic site, Ser293 of the active site, and Phe346 of surroundings of the active site. The other compounds also exhibited by similar H-bond interactions (Table S2). The structural resemblance of the isolated compounds leads to similar binding interactions with the protein molecule. The interactions of compounds with active site gorge and PAS might cause mixed-type inhibition.

4. Conclusion

Achyranthes bidentata Blume seeds are well-known functional foods for their nutritional composition and health benefits. However, knowledge regarding the bioactive compounds of the seeds remains scarce. Hence, this study explored the phytochemical profile of *A. bidentata* seeds using chemometric guided isolation approach. Chemometric analysis revealed the abundance of triterpenoid saponins in water and *n*-butanol fraction which led to the identification of fifty-six compounds from the different extract/ fractions of *A. bidentata* seed. Considering chemometrics observations, water fraction was targeted for the isolation of new triterpenoid saponins, which resulted in the isolation of two previously undescribed (**1**, **2**) along with three previously known triterpenoid, (**3-5**). All the isolated compounds have shown significant AChE inhibitory activity and mixed-type of inhibition kinetics. *In silico* study provided information about the binding interactions of pure compounds with the active and peripheral anionic sites.

Moreover, the estimated binding energies of isolated compounds indicated greater stability of the enzyme-inhibitor complex. Overall, the chemometric-guided isolation approach provides

an excellent strategy for dereplicating and isolating new compounds. Thus, further in-depth investigation of highly unexplored seeds of *A. bidentata* is crucial for their development as alternative cereal grains and for discovering new compounds.

CRediT authorship contribution statement

Shivani Puri: Methodology, Investigation, Formal analysis, Writing – original draft. **Prithvi Pal Singh**: Formal analysis, Writing – original draft. **Prateek Singh Bora**: Formal analysis, Writing – original draft. **Upendra Sharma**: Conceptualization, Formal analysis, Supervision, Writing - review & editing, Funding acquisition.

Declaration of interest

The authors declare that they have no conflict of interest.

Acknowledgment

The authors thank the Director, CSIR-IHBT, for continuous encouragement and support. Shivani Puri is thankful to CSIR for the GPAT-JRF fellowship.

Supplementary material

The supplementary data of the manuscript is available in Table S1, S2 and Figure S1-S38.

References

Anokwuru, C. P., Sandasi, M., Chen, W., van Vuuren, S., Elisha, I. L., Combrinck, S., & Viljoen, A. M. (2021). Investigating antimicrobial compounds in South African Combretaceae species using a biochemometric approach. *Journal of Ethnopharmacology*, *269*, 113681. https://doi.org/10.1016/j.jep.2020.113681

Ballantyne, M., McCabe, P., & Murray, R. (1971). Claisen rearrangements—II: Synthesis of six natural coumarins. *Tetrahedron, 27*(4), 871-877. https://doi.org/10.1016/S0040-4020(01)92484-6

Bora, P. S., Agrawal, P., Kaushik, N. K., Puri, S., Sahal, D., & Sharma, U. (2023). Antiplasmodial activity of the bulbs of *Fritillaria cirrhosa* D. Don (Syn: *Fritillaria roylei* Hook.): UPLC-IM-Q-TOF-MS/MS-based biochemometric approach for the identification of marker compounds. *Journal of Ethnopharmacology, 310*, 116389. https://doi.org/10.1016/j.jep.2023.116389.

Cao, Y., Gu, C., Zhao, F., Tang, Y., Cui, X., Shi, L., Xu, L., & Yin, L. (2017). Therapeutic effects of *Cyathula officinalis* Kuan and its active fraction on acute blood stasis rat model and identification constituents by HPLC-QTOF/MS/MS. *Pharmacognosy Magazine, 13*(52), 693. https://doi.org/10.4103%2Fpm.pm_560_16

Chen, C.-Y., Chang, F.-R., Yen, H.-F., & Wu, Y.-C. (1998). Amides from stems of *Annona cherimola*. *Phytochemistry, 49*(5), 1443-1447. https://doi.org/10.1016/S0031-9422(98)00123-X

Dong, Q., Yan, J., Zheng, M., Huai, H., & Tan, J. (2010). Chemical constituents from seeds of *Achyranthes bidentata* Blume. *Journal of Tropical and Subtropical Botany, 18*(5), 569-572. http://xuebao.scib.ac.cn

Dvir, H., Silman, I., Harel, M., Rosenberry, T. L., & Sussman, J. L. (2010). Acetylcholinesterase: from 3D structure to function. *Chemico-Biological Interactions, 187*(1-3), 10-22. https://doi.org/10.1016/j.cbi.2010.01.042

Ellman, G. L., Courtney, K. D., Andres Jr, V., & Featherstone, R. M. (1961). A new and rapid colorimetric determination of acetylcholinesterase activity. *Biochemical Pharmacology, 7*(2), 88-95. https://doi.org/10.1016/0006-2952(61)90145-9

Fu, J., Wu, H., Wu, H., Deng, R., & Li, F. (2019). Chemical and metabolic analysis of *Achyranthes bidentate* saponins with intestinal microflora-mediated biotransformation by ultra-performance liquid chromatography-quadrupole time-of-flight mass spectrometry coupled with metabolism platform. *Journal of Pharmaceutical and Biomedical Analysis, 170*, 305-320. https://doi.org/10.1016/j.jpba.2019.03.041

Greger, H., Hofer, O., & Nikiforov, A. (1982). New sesquiterpene-coumarin ethers from *Achillea* and *Artemisia* species. *Journal of Natural Products, 45*(4), 455-461. https://doi.org/10.1021/np50022a017

Harborne, J. B., & Williams, C. A. (1984). 6-Hydroxyflavones and other flavonoids of Crocus. *Zeitschrift für Naturforschung C, 39*(1-2), 18-23. https://doi.org/10.1515/znc-1984-1-204

He, X., Wang, X., Fang, J., Chang, Y., Ning, N., Guo, H., Huang, L., & Huang, X. (2017). The genus *Achyranthes*: A review on traditional uses, phytochemistry, and pharmacological activities. *Journal of Ethnopharmacology, 203*, 260-278. https://doi.org/10.1016/j.jep.2017.03.035

Hikino, H., Arihara, S., & Takemoto, T. (1969). Ponasteroside A, a glycoside of insect metamorphosing substance from *Pteridium aquilinum* var. latiusculum:: Structure and absolute configuration. *Tetrahedron, 25*(17), 3909-3917. https://doi.org/10.1016/S0040-4020(01)82923-9

Kinjo, J., Suyama, K., & Nohara, T. (1995). Triterpenoidal saponins from *Dumasia truncata*. *Phytochemistry, 40*(6), 1765-1767. https://doi.org/10.1016/0031-9422(95)00545-I

Li, Y. J., Wei, H. L., Qi, L. W., Chen, J., Ren, M. T., & Li, P. (2010). Characterization and identification of saponins in *Achyranthes bidentata* by rapid-resolution liquid chromatography with electrospray ionization quadrupole time-of-flight tandem mass

spectrometry. *Rapid Communications in Mass Spectrometry*, *24*(20), 2975-2985. https://doi.org/10.1002/rcm.4728

Ling, Y., Li, Z., Chen, M., Sun, Z., Fan, M., & Huang, C. (2013). Analysis and detection of the chemical constituents of Radix Polygalae and their metabolites in rats after oral administration by ultra high-performance liquid chromatography coupled with electrospray ionization quadrupole time-of-flight tandem mass spectrometry. *Journal of Pharmaceutical and Biomedical Analysis*, *85*, 1-13. https://doi.org/10.1016/j.jpba.2013.06.011

Ma, Q., Cai, S., Liu, X., Shi, J., & Yi, J. (2021). Characterization of phytochemical components and identification of main antioxidants in *Crateva unilocalaris* Buch. shoots by UHPLC-Q-Orbitrap-MS2 analysis. *Food Research International*, *143*, 110264. https://doi.org/10.1016/j.foodres.2021.110264

Mai, N. T., Anh, B. T. M., Xuan, V. T., Lan, H. T. T., Yen, D. T. H., Tai, B. H., Nhiem, N. X., & Van Kiem, P. (2023). Achyranbidens A–C: three new compounds from *Achyranthes bidentata* Blume. *Natural Product Research*, 1-10. https://doi.org/10.1080/14786419.2023.2174534

Marcone, M. F., Jahaniaval, F., Aliee, H., & Kakuda, Y. (2003). Chemical characterization of *Achyranthes bidentata* seed. *Food Chemistry*, *81*(1), 7-12. https://doi.org/10.1016/S0308-8146(02)00250-9

Memon, A. A., Memon, N., Bhanger, M. I., & Luthria, D. L. (2013). Assay of phenolic compounds from four species of ber (*Ziziphus mauritiana* L.) fruits: comparison of three base hydrolysis procedure for quantification of total phenolic acids. *Food Chemistry*, *139*(1-4), 496-502. https://doi.org/10.1016/j.foodchem.2013.01.065

Mi, Y. G., Xu, X. Y., Hong, L. L., Jiang, M. T., Chen, B. X., Li, X. H., Wang, H. D., Zou, Y. D., Zhao, X., & Li, Z. (2023). Comparative Characterization of the Ginsenosides from

555 Six Panax Herbal Extracts and Their In Vitro Rat Gut Microbial Metabolites by
556 Advanced Liquid Chromatography–Mass Spectrometry Approaches. *Journal of*
557 *Agricultural and Food Chemistry*. https://doi.org/10.1021/acs.jafc.3c01093
558 Mikołajczyk-Bator, K., Błaszczyk, A., Czyżniejewski, M., & Kachlicki, P. (2016a).
559 Characterisation and identification of triterpene saponins in the roots of red beets (*Beta*
560 *vulgaris* L.) using two HPLC–MS systems. *Food Chemistry, 192,* 979-990.
561 https://doi.org/10.1016/j.foodchem.2015.07.111
562 Mikołajczyk-Bator, K., Błaszczyk, A., Czyżniejewski, M., & Kachlicki, P. (2016b).
563 Identification of saponins from sugar beet (*Beta vulgaris*) by low and high-resolution
564 HPLC–MS/MS. *Journal of Chromatography B, 1029*, 36-47.
565 https://doi.org/10.1016/j.jchromb.2016.06.038
566 Mizui, F., Kasai, R., Ohtani, K., & Tanaka, O. (1990). Saponins from bran of quinoa,
567 *Chenopodium quinoa* Willd. II. *Chemical and Pharmaceutical Bulletin*, *38*(2), 375-
568 377. https://doi.org/10.1248/cpb.38.375
569 Oulad-Ali, A., Guillaume, D., Weniger, B., Jiang, Y., & Anton, R. (1994). Mabiosides CE:
570 triterpenoid saponins from the bark of *Colubrina elliptica*. *Phytochemistry*, *36*(2), 445-
571 448. https://doi.org/10.1016/S0031-9422(00)97092-4
572 Pluskal, T., Castillo, S., Villar-Briones, A., & Orešič, M. (2010). MZmine 2: modular
573 framework for processing, visualizing, and analyzing mass spectrometry-based
574 molecular profile data. *BMC Bioinformatics*, *11*(1), 1-11. https://doi.org/10.1186/1471-
575 2105-11-395
576 Sá, I. S., da Silva, F. M., & de CS Nunomura, R. (2022). Simplex centroid mixture design, DI-
577 ESI-MS, and chemometric analysis-guided isolation of parinarioidin C from bark of
578 *Brosimum parinarioides* (Moraceae). *Phytochemistry Letters, 50,* 25-30.
579 https://doi.org/10.1016/j.phytol.2022.04.002

580 Saboury, A. (2009). Enzyme inhibition and activation: a general theory. *Journal of the Iranian*
581 *Chemical Society*, *6*, 219-229. https://doi.org/10.1007/BF03245829
582 Wang, Y., Yao, C., Wang, M., Li, J., Li, Z., Zhang, J., Wei, W., Bi, Q., & Guo, D. a. (2022).
583 Systematical characterization and comparison of saponins in *Achyranthes bidentata*
584 Blume and its three analogous species. *Phytochemical Analysis*, *33*(5), 766-775.
585 https://doi.org/10.1002/pca.3128
586 Warashima, T., Miyase, T., & Ueno, A. (1991). Novel acylated saponins from *Tragopogon*
587 *porrifolius* L. Isolation and the structures of tragopogonsaponins AR. *Chemical and*
588 *Pharmaceutical Bulletin*, *39*(2), 388-396. https://doi.org/10.1248/cpb.39.388
589 Wong, C. Y., Leong, K. H., He, X., Zheng, F., Sun, J., Wang, Z., Heh, C. H., & Kong, K. W.
590 (2022). Phytochemicals of six selected herbal plants and their inhibitory activities
591 towards free radicals and glycation. *Food Bioscience*, *46*, 101557.
592 https://doi.org/10.1016/j.fbio.2022.101557
593 Yannai, S. (2003). *Dictionary of Food Compounds with CD-ROM: Additives, Flavors, and*
594 *Ingredients.* (1st Edition ed.). New York: Chapman & Hall/CRC, Boca Raton.
595 Yaoita, Y., Amemiya, K., Ohnuma, H., Furumura, K., Masaki, A., Matsuki, T., & Kikuchi, M.
596 (1998). Sterol constituents from five edible mushrooms. *Chemical and Pharmaceutical*
597 *Bulletin*, *46*(6), 944-950. https://doi.org/10.1248/cpb.46.944
598 Yi, J., Li, X., Wang, S., Wu, T., & Liu, P. (2022). Steam explosion pretreatment of *Achyranthis*
599 *bidentatae* radix: Modified polysaccharide and its antioxidant activities. *Food*
600 *Chemistry*, *375*, 131746. https://doi.org/10.1016/j.foodchem.2021.131746
601 Ying-Ying, W., Jia-Yuan, L., Chang-Liang, Y., Zhang, J.-Q., Yang, Y., Shuai, Y., Min, G.,
602 Shi-Fei, W., Wen-Long, W., & Qi-Rui, B. (2022). Deep chemical identification of
603 phytoecdysteroids in *Achyranthes bidentata* Blume by UHPLC coupled with linear ion

trap-Orbitrap mass spectrometry and targeted isolation. *Chinese Journal of Natural Medicines, 20*(7), 551-560. https://doi.org/10.1016/S1875-5364(22)60185-7

Yoshikawa, M., Morikawa, T., Asao, Y., Fujiwara, E., Nakamura, S., & Matsuda, H. (2007). Medicinal flowers. XV. The structures of noroleanane-and oleanane-type triterpene oligoglycosides with gastroprotective and platelet aggregation activities from flower buds of *Camellia japonica*. *Chemical and Pharmaceutical Bulletin, 55*(4), 606-612. https://doi.org/10.1248/cpb.55.606

Yoshikawa, M., Murakami, T., Kadoya, M., Matsuda, H., Muraoka, O., Yamahara, J., & Murakami, N. (1996). Medicinal foodstuffs. III. Sugar beet.(1): Hypoglycemic oleanolic acid oligoglycosides, betavulgarosides, I, II, III, and IV, from the root of *Beta vulgaris* L.(Chenopodiaceae). *Chemical and Pharmaceutical Bulletin, 44*(6), 1212-1217. https://doi.org/10.1248/cpb.44.1212

Yoshikawa, M., Murakami, T., Ueno, T., Hirokawa, N., Yashiro, K., Murakami, N., Yamahara, J., Matsuda, H., Saijoh, R., & Tanaka, O. (1997). Bioactive saponins and glycosides. IX. Notoginseng (2): structures of five new dammarane-type triterpene oligoglycosides, notoginsenosides-E,-G,-H,-I, and-J, and a novel acetylenic fatty acid glycoside, notoginsenic acid β-sophoroside, from the dried root of *Panax notoginseng* (Burk.) FH Chen. *Chemical and Pharmaceutical Bulletin, 45*(6), 1056-1062. https://doi.org/10.1248/cpb.45.1056

Yuan, W., Wang, P., Zhang, Z., Su, Z., & Li, S. (2013). Triterpenoid saponins from *Sesbania vesicaria*. *Phytochemistry Letters, 6*(1), 106-109. https://doi.org/10.1016/j.phytol.2012.11.003

Zhang, S., Zhang, Q., Zhang, D., Wang, C., & Yan, C. (2018). Anti-osteoporosis activity of a novel *Achyranthes bidentata* polysaccharide via stimulating bone formation. *Carbohydrate polymers, 184*, 288-298. https://doi.org/10.1016/j.carbpol.2017.12.070

Figure and Table legends:

Figure 1 (A) PCA score plot of the UPLC-IM-Q-TOF-MS/MS data of extract and fractions of *A. bidentata* seeds in negative ionization mode; (B) Loading plot for the LC-MS profile in negative ionization mode; (C) Variable trend plot of characteristic mass ions and (D) Contribution plot of water fraction versus average data set of the model; Bars marked in red from left to right represents *m/z* 925, 939, 955, 925, 1101, 1087, 823, 579, 421, respectively.

Figure 2 The MS/MS fragmentation pathways of identified compounds at, (a) peak 17 (b) peak 21 (c) peak 15 and (d) peak 2.

Figure 3 (A) Chemical structure of isolated compounds (1-5) and (B) Key HMBC (→), ^{1}H-^{1}H COSY (▬) and NOESY (↔) correlations of compound 1 and 2.

Figure 4 (A) % inhibition plot of isolated compounds (**1-5**); (B) Lineweaver Burk plots of acetylcholinesterase inhibition kinetics by isolated compounds (1-5) and (C) 2-D interaction diagram of compound 1 (a) & 2 (b). The (→) indicate H-bond interactions.

Table 1. UPLC-IM-Q-TOF-MS/MS based identification of different compounds in the extract and fractions of *A. bidentata* seeds.

Table 2. ^{1}H (600MHz) and ^{13}C (150MHz) data of compound 1 & 2 in CD_3OD.

Fig. 1

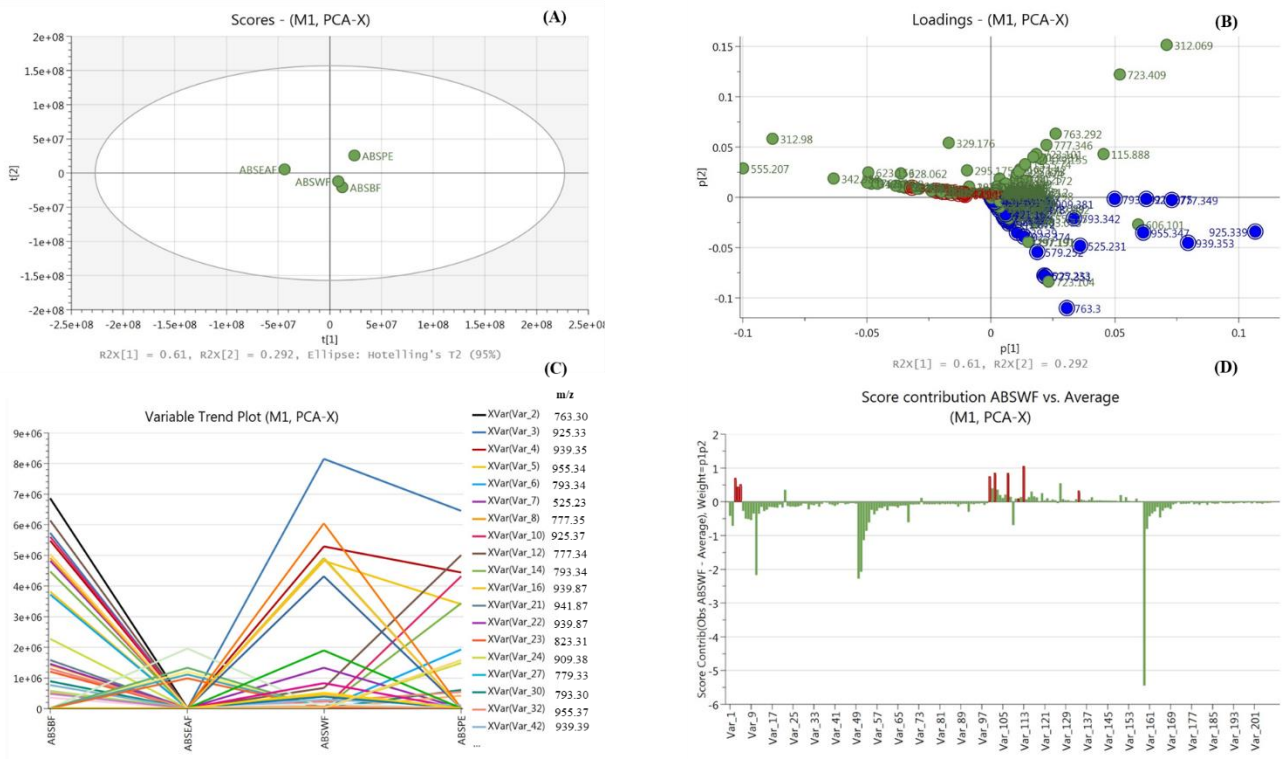

Fig. 2

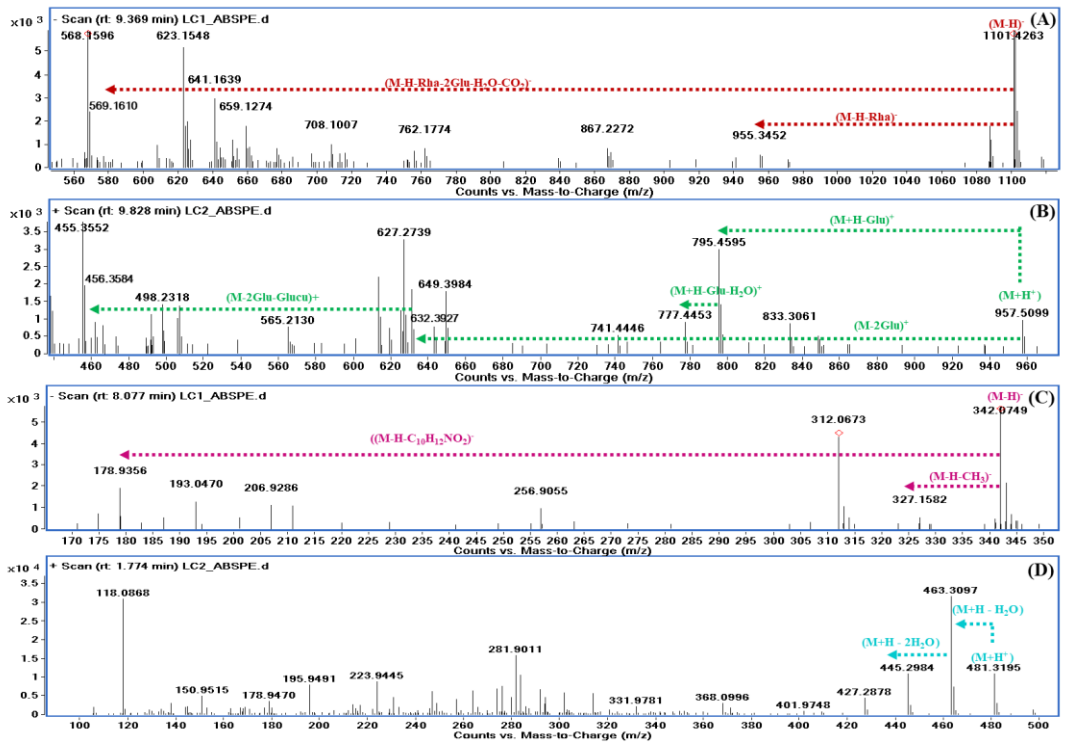

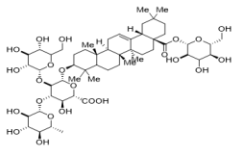

3-O-[beta-D-glucopyranosyl-(1-2)-alpha-L-rhamnopyranosyl- (1-3)-beta-D-glucuronopyranosyl]-28-O-beta-D-glucopyranosyl oleanolic acid

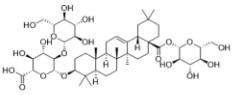

Ginsenoside Ro

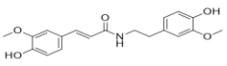

N-trans-Feruloyl-3-methoxytyramine

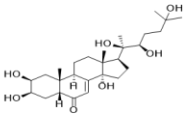

20-Hydroxyecdysone

684

685

686 **Fig. 3**

(A)

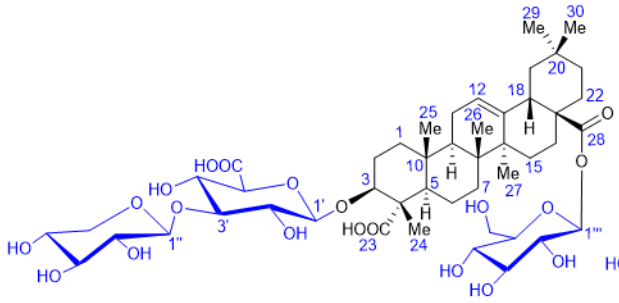

1

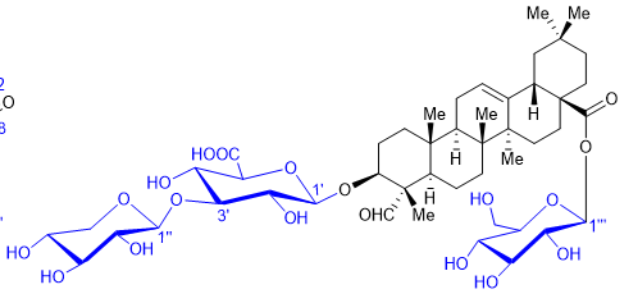

2

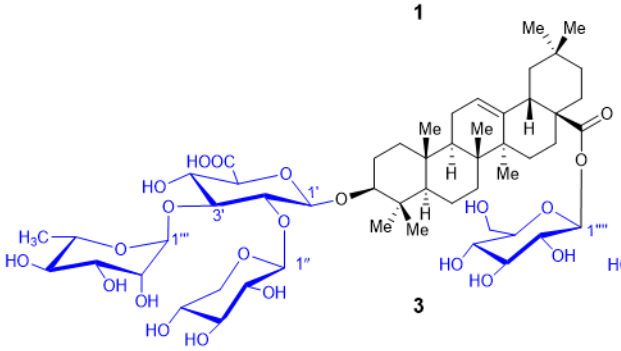

3

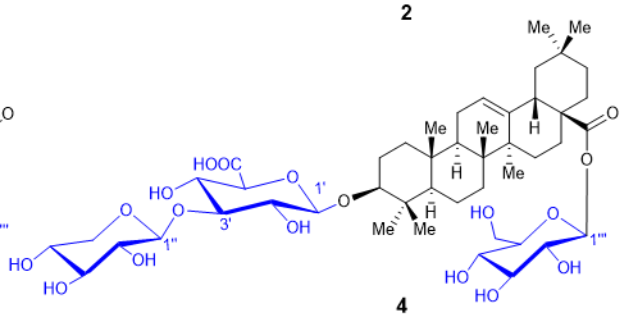

4

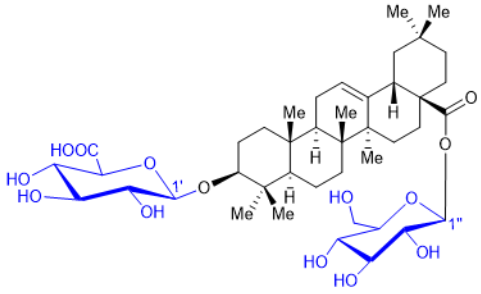

5

(B)

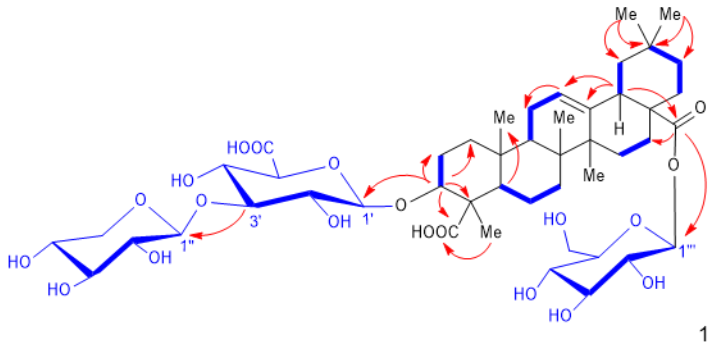

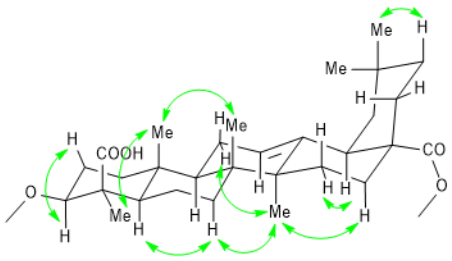

1

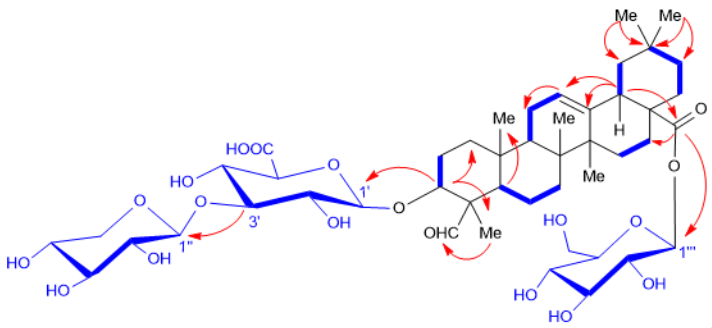

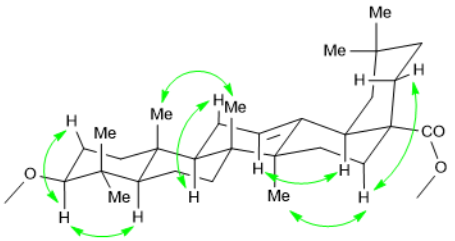

2

687

688

Fig. 4

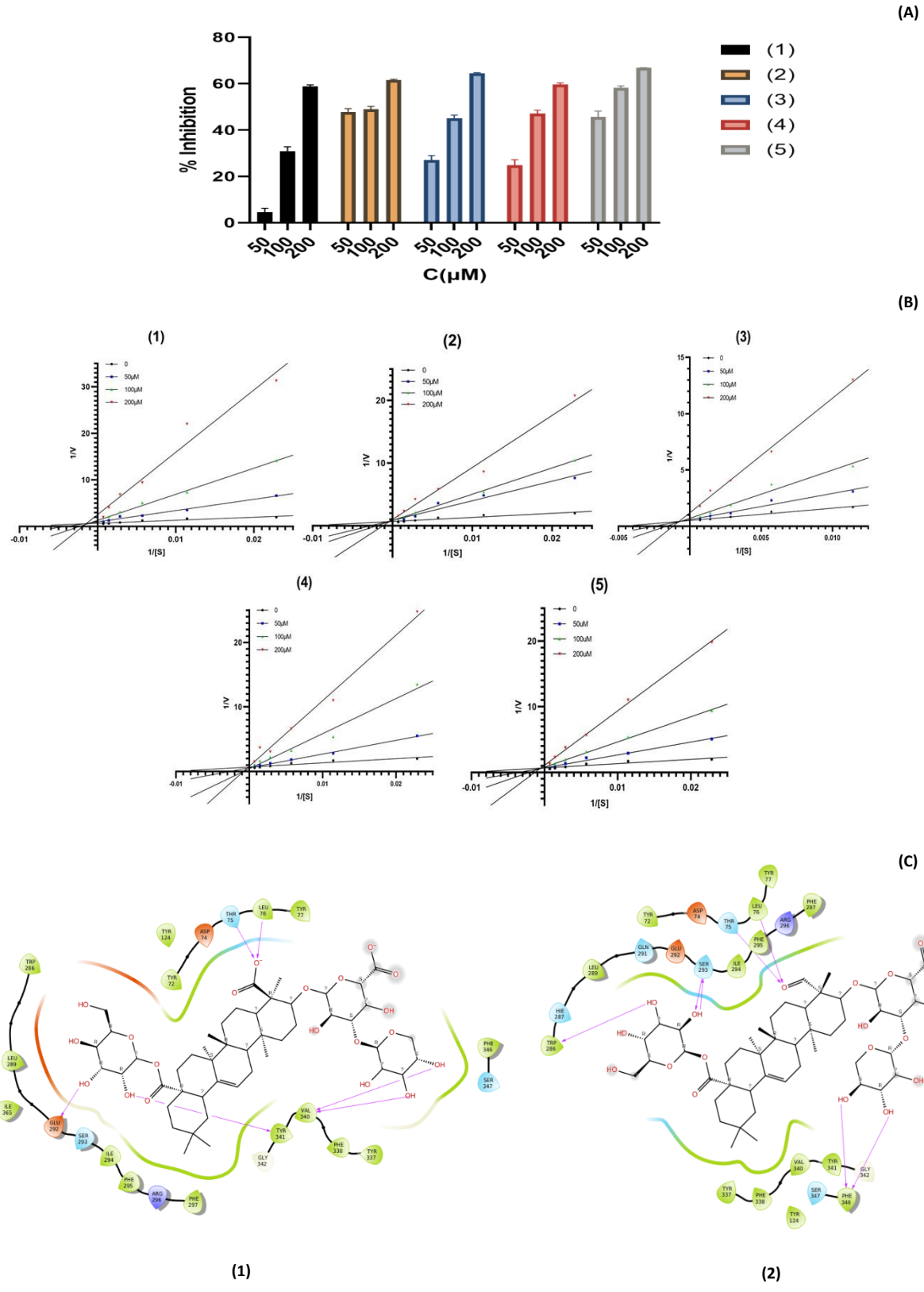

Peak no	Rt (min)	Molecular formula	Observed *m/z* value	Adduct		Fragment ions	Compound name	Class of compound	ABSPE	ABSEAF	ABSWF	ABSBF	References
				Negative mode	Positive mode								
1	1.461	$C_{24}H_{22}O_{15}$	549.0869	$(M-H)^-$		549.0869 $(M-H)^-$, 505.0831$(M-H-CO_2)^-$, 301.0265 (M-H-(6-O-Malonyl-β-D-glucoside$(C_9H_{13}O_8)^-$	Quercetin 3-O-(6-O-malonyl-*β*-D-glucoside	Flavonoid glycoside	+	+	+	+	(Memon, Memon, Bhanger, & Luthria, 2013)
2	1.774	$C_{27}H_{44}O_7$	481.3195		$(M+H)^+$	481.3195 $(M+H)^+$, 463.3097 $(M+H-H_2O)^+$, 445.2984 $(M+H-2H_2O)^+$	20-Hydroxyecdysone	Ecdysteroid	+	+	+	+	(He, Wang, Fang, Chang, Ning, Guo, et al., 2017)
3	2.073	$C_{26}H_{34}O_6$	487.2307	$(M+HCOO)^-$		487.2307 $(M+HCOO)^-$, 477.0311 $(M+Cl^{35})^-$, 247.0673, 203.0460	Pectachol	Coumarin	+	-	-	-	(Greger, Hofer, & Nikiforov, 1982)
4	2.194	$C_{27}H_{44}O_7$	525.2297	$(M+HCOO)^-$		525.2297 $(M+HCOO)^-$, 479.0237 $(M-H)^-$, 159.0260 $(M+HCOO^- - C_{19}H_{28}O_4)$	25S-Inokosterone	Ecdysteroid	+	+	+	+	(Ying-Ying, Jia-Yuan, Chang-Liang, Zhang, Yang, Shuai, et al., 2022)
5	5.006	$C_{42}H_{74}O_{16}$	879.4697	$(M-H+HCOO)^-$		879.4697 $(M-H+HCOO)^-$, 833.4268 $(M-H)^-$, 671.0942 $(M-H-glu)^-$, 509.0512 $(M-H-2Glu)^-$	Notoginsenoside J	Triterpenoid saponin	+	-	-	-	(Yoshikawa, Murakami, Ueno, Hirokawa, Yashiro, Murakami, et al., 1997)
6	5.038	$C_{27}H_{44}O_7$	481.3193		$(M+H)^+$	481.3193 $(M+H)^+$, 463.3089$(M+H-H_2O)^+$, 445.2979 $(M+H-2H_2O)^+$	25R-Inokosterone	Ecdysteroid	+	+	+	+	(Ying-Ying, et al., 2022)
7	5.189	$C_{41}H_{60}O_{15}$	791.3877	$(M-H)^-$		791.3877 $(M-H)^-$, 631.0815 $(M-H-Diox)^-$	Betavulgaroside II	Triterpenoid saponin	+	-	+	-	(Yoshikawa, Murakami, Kadoya, Matsuda, Muraoka, Yamahara, et al., 1996)
8	5.219	$C_{21}H_{20}O_{11}$	449.1097		$(M+H)^+$	449.1097 $(M+H)^+$, 287.0564 $(M+H-Glu)^+$, 195.9489 (M+H-Glu-Phenol substituent)$^+$	Scutellarein 7-glucoside	Flavonoid glycoside	+	-	-	+	(Harborne & Williams, 1984)
9	5.499	$C_{43}H_{68}O_{15}$	823.4494	$(M-H)^-$		823.4494 $(M-H)^-$, 485.0923 $(M-H-2Glu-CH_2)^-$	Yiamoloside B	Triterpenoid saponin	+	-	-	-	(Wong, Leong, He, Zheng, Sun, Wang, et al., 2022)
10	5.561	$C_{47}H_{81}O_{19}$	949.5587	$(M-H)^-$		949.5587 $(M-H)^-$, 817.1150 $(M-H-Ara)^-$, 493.0574 $(M-H-Ara-2Glu)^-$	Notoginsenoside NL-E_1	Triterpenoid saponin	+	-	+	-	(Mi, Xu, Hong, Jiang, Chen, Li, et al., 2023)
11	6.105	$C_{17}H_{17}NO_4$	300.1258		$(M+H)^+$	300.1258 $M+H)^+$, 178.0588 (M-(4-hydroxyphenyl) ethyl)$^+$	N-cis-caffeoyltyramine	Phenolic acid	+	+	-	+	(Chen, Chang, Yen, & Wu, 1998)
12	6.301	$C_{29}H_{48}O_7$	509.3494		$(M+H)^+$	509.3494 $(M+H)^+$, 327.1708	Amarasterone B	Ecdysteroid	+	+	-	-	(Cao, Gu, Zhao, Tang, Cui, Shi, et al., 2017)
13	6.941	$C_{18}H_{19}NO_4$	314.1410		$(M+H)^+$	336.1221 $(M+Na^+)^+$, 314.1410 $(M+H)^+$,177.0555 (M+H-(4-hydroxyphenyl) ethyl($C_8H_{10}O$) - CH_3))$^+$	N-cis-feruloyltramine	Phenolic acid	+	+	+	+	(Cao, et al., 2017)

14	7.581	$C_{18}H_{19}NO_4$	314.1421		$(M+H)^+$	336.1232 $(M+Na^+)^+$,314.1421 $(M+H)^+$, 177.0556 (M+H- $C_8H_{10}O$[4-hydroxyphenyl) ethyl]- CH_3^+)	N-trans-feruloyltramine	Phenolic acid	+	+	+	+	(Cao, et al., 2017)
15	8.077	$C_{19}H_{21}NO_5$	342.0749	$(M-H)^-$		342.0749 $(M-H)^-$, 327.1582 (M-H-$CH_3)^-$, 178.9356(M-H-$C_9H_{10}NO_2$[2-(4-hydroxy-3-methoxyphenyl) ethyl])$^-$	N-trans-feruloyl-3-methoxytyramine	Phenolic acid	+	+	+	+	(Cao, et al., 2017)
16	8.754	$C_{47}H_{74}O_{19}$	941.3632	$(M-H+O)^-$		941.3632 $(M-H+O)^-$, 471.0763 (M-H-Glu-Ara-Glucu+O)$^-$	Chikusetsusaponin IV+O	Triterpenoid saponin	+	-	+	+	(Fu, Wu, Wu, Deng, & Li, 2019)
17	9.369	$C_{54}H_{86}O_{23}$	1101.4263	$(M-H)^-$		1101.4263 $(M-H)^-$, 955.3452 (M-H-Rha)$^-$, 569.1610 (M-H-Rha-2Glu-H_2O-$CO_2)^-$	3-O-[β-D-glucopyranosyl-(1→2) -α-L-rhamnopyranosyl-(1→3)-β-D-glucuronopyranosyl]-28-O-β-D-glucopyranosyl oleanolic acid	Triterpenoid saponin	+	-	+	+	(Cao, et al., 2017)
18	9.490	$C_{33}H_{54}O_{12}$	641.1635	$(M-H)^-$		687.1820 $(M-H+HCOO)^-$, 641.1635 $(M-H)^-$, 479.1219(M-H-Glu)$^-$	25R-inkosterone-Glucose	Ecdysteroid	+	+	-	+	(Ying-Ying, et al., 2022)
19	9.608	$C_{33}H_{54}O_{12}$	641.1640	$(M-H)^-$		641.1640 $(M-H)^-$, 479.1230 $(M-Glu)^-$	β-Ecdysterone-Glucose	Ecdysteroid	+	+	-	+	(Ying-Ying, et al., 2022)
20	9.671	$C_{52}H_{80}O_{24}$	1087.4104	$(M-H)^-$		1087.4104 $(M-H)^-$, 955.3795 (M-H-Xyl)$^-$, 793.3378 (M-H-Xyl-$C_5H_6O_6)^-$, 613.1647 (M-H-Xyl-$C_5H_6O_6$ -Glu-$H_2O)^-$	Unknown	Triterpenoid saponin	+	-	+	+	-
21	9.795	$C_{42}H_{66}O_{14}$	795.4571		$(M+H)^+$	795.4571 $(M+H)^+$, 632.3920 $(M-Glu)^+$, 456.3588 $(M-Glu-Glucu)^+$	Zingibroside R1	Triterpenoid saponin	+	-	+	+	(Li, Wei, Qi, Chen, Ren, & Li, 2010)
22	9.828	$C_{48}H_{76}O_{19}$	957.5099		$(M+H)^+$	957.5099 $(M+H)^+$, 795.4595 $(M+H-Glu)^+$,632.3927(M-2Glu)+ , 456.3584 $(M-2Glu-Glucu)^+$	Ginsenoside Ro/ Chikusetsusaponin V	Triterpenoid saponin	+	-	+	+	(Li, Wei, Qi, Chen, Ren, & Li, 2010)
23	9.861	$C_{42}H_{66}O_{14}$	795.4585		$(M+H)^+$	795.4585 $(M+H)^+$, 632.3902 $(M-Glu)^+$ 456.3581 $(M-Glu-Glucu)^+$, 438.3472 $(M-Glu-Glucu-H_2O)^+$,	Chikusetsusaponin IVa	Triterpenoid saponin	+	-	+	+	(Li, Wei, Qi, Chen, Ren, & Li, 2010)
24	9.877	$C_{48}H_{76}O_{19}$	957.5134		$(M+H)^+$	957.5134 $(M+H)^+$, 811.4528 $(M+H-Rha)^+$, 649.3995 $(M+H-Rha-Glu)^+$, 473.3642 $(M+H-Rha-Glu-Glucu)^+$, 455.3561 $(M+H-Rha-Glu-Glucu-H_2O)^+$,	Unknown	Triterpenoid saponin	+	-	+	-	-
25	10.039	$C_{47}H_{73}O_{19}$	941.3639	$(M-H)^-$		941.3639 $(M-H)^-$, 809.3312 (M-H-Hex)$^-$, 717.1786 (M-H-Hex-H_2O-$CO_2)^-$	Hex-Pen-UrA hederagenin	Triterpenoid saponin	+	+	+	+	(Mikołajczyk-Bator, Błaszczyk, Czyżniejewski, & Kachlicki, 2016a)
26	10.222	$C_{47}H_{72}O_{20}$	979.4557		$(M+Na^+)^+$	979.4557 $(M+Na^+)^+$, 974.5042 $(M+NH_4^+)^+$, 817.4028 $(M+Na^+$-$C_5H_6O_6)^+$, 812.4495 $(M+NH_4^+$-$C_5H_6O_6)^+$, 795.4225 $(M+H-Glu)^+$, 456.3584 $(M+H-Glu-C_5H_6O_6$-$Glucu)^+$	Achyranthoside C	Triterpenoid saponin	+	-	+	+	(Li, Wei, Qi, Chen, Ren, & Li, 2010)

27	10.223	$C_{47}H_{72}O_{20}$	955.3440 974.5035	$(M-H)^-$	$(M+NH_4)^+$	955.3440 $(M-H)^-$, 823.3111 (M-H-Xyi)$^-$, 601.1652 (M-H-Xyl-Glucu-H_2O-CO)$^-$ 974.5035 $(M+NH_4)^+$, 957.4721 $(M+H)^+$, 812.4495 $(M+NH_4$-Glu$)^+$, 795.4207 (M+H-Glu)$^+$, 663.3768 (M+H-Glu-Xyl)$^+$, 487.3451 (M+H-Glu-Xyl-Glucu)$^+$	Unknown	Triterpenoid saponin	+	-	+	-	-
28	10.348	$C_{53}H_{83}O_{23}$	1087.4096	$(M-H)^-$		1087.4096 $(M-H)^-$, 955.3422(M-H-Hex)$^-$, 793.3375 ((M-H-Hex-Hex)$^-$	Hex-Hex-Pen-UrA oleanolic acid	Triterpenoid saponin	+	+	+	+	(Mikołajczyk-Bator, Błaszczyk, Czyżniejewski, & Kachlicki, 2016a)
29	10.407	$C_{48}H_{78}O_{18}$	941.3611	$(M-H)^-$		977.3212 $(M+Cl^{35})^-$, 941.3611 $(M-H)^-$	Oleanolic acid 28-O-*β*-D gluco-pyranoside-3-O-[*β*-D-glucopyranosyl-(1→3)-*β*-D galacto-pyranoside)	Triterpenoid saponin	+	-	+	+	(Mai, Anh, Xuan, Lan, Yen, Tai, et al., 2023)
30	10.841	$C_{47}H_{72}O_9$	939.3484 963.4537	$(M-H)^-$	$(M+Na)^+$	939.3484 $(M-H)^-$, 807.3173 (M-H-Xyl)$^-$, 963.4537 $(M+Na^+)^+$, 779.4652 (M+H-Glu)$^+$, 471.3501 (M+H-Glu-Xyl-Glucu)$^+$,453.3388 (M+H-Glu-Xyl-Glucu-$H_2O)^+$	Unknown	Triterpenoid saponin	+	-	+	-	-
31	10.960	$C_{53}H_{84}O_{22}$	1095.5386		$(M+Na)^+$	1095.5386 $(M+Na^+)^+$, 765.4488 (M+H-Rha-Glu)$^+$, 633.4023 (M+H-Rha-Glu-Xyl)$^+$, 457.3692 (M+H-Rha-Glu-Xyl-Glucu)$^+$, 439.3604 (M+H-Rha-Glu-Xyl-Glucu-$H_2O)^+$	3-O-[*β*-D-xylo-pyranosyl-(1→2)]-[*a*-L-rhamno-pyranosyl-(1→3)]-*β*-D-glucurono-pyranosyl-28-O-*β*-D-glucopyransoyl-3*β*-hydroxy-olean-12-en-28-oate.	Triterpenoid saponin	+	-	+	+	(Kinjo, Suyama, & Nohara, 1995)
32	10.966	$C_{41}H_{59}O_{16}$	807.3155	$(M-H)^-$		807.3155 $(M-H)^-$, 627.1788 (M-H-Acetyl-$H_2O)^-$	Acetyl uronic acid gypsogenin	Triterpenoid saponin	+	-	+	-	(Mikołajczyk-Bator, Błaszczyk, Czyżniejewski, & Kachlicki, 2016b)
33	11.616	$C_{47}H_{74}O_{18}$	944.5274		$(M+NH_4)^+$	944.5274 $(M+NH_4)^+$, 812.4840 $(M+NH_4$-Ara$)^+$, 633.4047 (M+H-Ara-Glu)$^+$, 456.3600 (M+H-Ara-Glu-Glucu)$^+$	Chikusetsusaponin IV	Triterpenoid saponin	+	-	+	+	(Li, Wei, Qi, Chen, Ren, & Li, 2010)
34	12.066	$C_{75}H_{112}O_{36}$	1587.7272	$(M-H)^-$		1587.7272 $(M-H)^-$, 925.3720 (M-H-Agly-3-O-β-D-Glucoside)$^-$, 793.3399 (M-H-Agly-(3-O-β-D-Glucoside)- (β-D-apiofuranose))$^-$, 485.1664((M-H-Agly-(3-O-β-D-Glucoside)- (β-D-apiofuranose)-Ara-Xyl-$CH_2O)^-$	Onjisaponin F	Triterpenoid saponin	+	-	-	+	(Ling, Li, Chen, Sun, Fan, & Huang, 2013)

35	12.125	$C_{53}H_{82}O_{25}$	1117.5045	$(M-H)^-$		1117.5045 $(M-H)^-$, 955.3419 $(M-H-C_5H_6O_6)^-$, 793.3399 $(M-H-C_5H_6O_6-Glu)^-$	Achyranthoside D/ Betavulgaroside V	Triterpenoid saponin	+	-	-	+	(Li, Wei, Qi, Chen, Ren, & Li, 2010)
36	12.141	$C_{15}H_{16}O_4$	261.1108		$(M+H)^+$	261.1108 $(M+H)^+$, 247.1712 $(M+H-CH_2)^+$, 217.1964 $(M+H-CH_2-OCH_2)^+$	3-(1,1 Dimethyl-allyl) scopoletin	Hydroxy coumarin	+	+	+	+	(Ballantyne, McCabe, & Murray, 1971)
37	12.372	$C_{47}H_{70}O_{20}$	953.4063	$(M-H)^-$		953.4063 $(M-H)^-$, 997.3799 $(M-H+CO_2)^-$, 793.3358 $(M-H-CO_2-C_5H_4O_6)^-$	Achyranthoside B/ Betavulgaroside I	Triterpenoid saponin	+	-	+	+	(Wang, Yao, Wang, Li, Li, Zhang, et al., 2022)
38	12.879	$C_{42}H_{64}O_{14}$	793.4383		$(M+H)^+$	793.4383 $(M+H)^+$, 647.3832 $(M+H-Rha)^+$, 467.3034 $(M+H-Rha-Glu-H_2O)^+$, 439.3597 $(M+H-Rha-Glu-H_2O-2CH_2)^+$	Mabioside C	Diterpenoid glycoside	+	-	+	+	(Oulad-Ali, Guillaume, Weniger, Jiang, & Anton, 1994)
39	14.279	$C_{53}H_{82}O_{24}$	1101.4089	$(M-H)^-$		1101.4089 $(M-H)^-$, 925.3094 $(M-H-Glucu)^-$, 779.3260 $(M-H-Glucu-Rha)^-$, 647.2949 $(M-H-Glucu-Rha-Xyl)^-$, 485.1572 $(M-H-Glucu-Rha-Xyl-Glu)^-$,	Unknown	Triterpenoid saponin	+	-	+	-	-
40	14.588	$C_{46}H_{74}O_{14}$	909.3737	$(M+CH_3COO)^-$		909.3737 $(M+CH_3COO)^-$, 793.2965 $(M-H-C_4H_9(Butyl\ chain))^-$, 455.1905 $(M-H-C_4H_9(Butyl\ chain)-Glu-Glucu)^-$	Chikusetsusaponin-IVa butyl ester	Triterpenoid saponin	+	+	+	+	(Cao, et al., 2017)
41	15.077	$C_{16}H_{12}O_5$	285.0777		$(M+H)^+$	285.0777 $(M+H)^+$, 175.1241 $(M-C_6H_6-OCH_3)^+$	Wogonin	Flavonoid	+	-	+	+	(He, et al., 2017)
42	15.259	$C_{62}H_{90}O_{26}$	1249.5590	$(M-H)^-$		1249.5590$(M-H)^-$, 911.3840 $(M-H-Glucu-Glu)^-$, 793.3387 $(M-H-Glucu-Glu-C_8H_6O)^-$	Tragopogonsaponin N	Triterpenoid saponin	+	-	-	-	(Warashima, Miyase, & Ueno, 1991)
43	15.454	$C_{23}H_{38}O_6$	411.2751		$(M+H)^+$	411.2751 $(M+H)^+$, 393.3556 $(M+H-H_2O)^+$,249.1876 $(M+H-Glu)^+$	Sterol 3-β-D-glucoside	Steroidal glycoside	+	+	-	-	-
44	15.487	$C_{47}H_{74}O_{18}$	949.4661		$(M+Na^+)^+$	949.4661 $(M+Na^+)^+$, 633.4003 $(M+H-Xyl-Glu)^+$, 457.3708 $(M+H-Xyl-Glu-Glucu)^+$,	Momordin IIc	Triterpenoid saponin	+	-	+	+	(Mizui, Kasai, Ohtani, & Tanaka, 1990)
45	16.366	$C_{56}H_{80}O_{21}$	1133.5177	$(M+HCOO)^-$		1133.5177 $(M+HCOO)^-$, 794.3436 $(M+HCOO-Glucu-Glu)^-$, 776.3341 $(M+HCOO-Glucu-Glu-H_2O)^-$	Tragopogonsaponin F	Triterpenoid saponin	+	-	-	-	(Warashima, Miyase, & Ueno, 1991)
46	16.930	$C_{53}H_{82}O_{23}$	1087.5320		$(M+H)^+$	1087.5320 $(M+H)^+$, 600.4701 $(M-3Glu)^+$	Camellioside C	Triterpenoid saponin	+	-	-	+	(Yoshikawa, Morikawa, Asao, Fujiwara, Nakamura, & Matsuda, 2007)
47	17.106	$C_{48}H_{76}O_{18}$	939.3802	$(M-H)^-$		939.3802 $(M-H)^-$, 777.3457 $(M-H-Glu)^-$, 597.2127 $(M-H-Glu-Xyl-H_2O-HCHO)^-$, 579.2494 $(M-H-Glu-Xyl-HCHO-2H_2O)^-$	Pseudoginsenoside Rt1 methyl ester	Triterpenoid saponin	+	-	-	+	(Mi, et al., 2023)
48	17.168	$C_{47}H_{70}O_{23}S$	1079.4036	$(M+HCOO)^-$		1079.4036 $(M+HCOO)^-$, 793.3383 $(M-H-SO_3-C_5H_4O_6)^-$, 763.3257 $(M-H-SO_3-C_5H_4O_6-CH_2O)^-$	Sulfachyranthoside B	Triterpenoid saponin	+	-	+	+	(Wang, et al., 2022)
49	17.718	$C_{57}H_{82}O_{22}$	1117.5255	$(M-H)^-$		1117.5255 $(M-H)^-$, 779.3513 $(M-H-Glucu-Glu)^-$	Tragopogonsaponin D	Triterpenoid saponin	+	-	-	+	(Warashima, Miyase, & Ueno, 1991)

50	18.324	$C_{30}H_{48}O_3$	457.3686		$(M+H)^+$	457.3686 $(M+H)^+$, 411.3646 $(M+H-HCOOH)^+$, 439.3615 $(M+H-H_2O)^+$ 393.3557 $(M+H-H_2O-HCOOH)^+$	Oleanolic Acid	Triterpenoid	+	+	+	+	(Li, Wei, Qi, Chen, Ren, & Li, 2010)
51	18.516	$C_{42}H_{66}O_{13}$	777.3452	$(M-H)^-$		777.3452 $(M-H)^-$, 631.2989 $(M-H-Rha)^-$, 437.1512 $(M-H-Rha-Glucu-H_2O)^-$	3-O-[α-L-rhamnopyranosyl-(1→3)-β-D-glucuronopyranosyl] oleanolic acid	Triterpenoid saponin	+	-	+	+	(Cao, et al., 2017)
52	19.071	$C_{47}H_{70}O_{21}$	969.4520	$(M-H)^-$		969.4520 $(M-H)^-$, 925.4293 $(M-H-CO_2)^-$, 763.2938 $(M-H-CO_2-Glu)^-$	Achyranthoside B+O	Triterpenoid saponin	+	-	-	-	(Fu, Wu, Wu, Deng, & Li, 2019)
53	19.255	$C_{41}H_{64}O_{13}$	763.2957	$(M-H)^-$		763.2957 $(M-H)^-$, 551.2202	28-Deglucosyl chikusetsusaponin IV	Triterpenoid saponin	+	-	+	+	(Ma, Cai, Liu, Shi, & Yi, 2021)
54	19.325	$C_{33}H_{56}O_{14}$	677.3767		$(M+H)^+$	677.3767 $(M+H)^+$, 370.3615 $(M+H-2Rha-CH_3)^+$, 352.3439 $(M+H-2Rha-CH_3-H_2O)^+$	(S)-Nerolidol 3-O-[α-L-Rhamno-pyranosyl-(1→4)-α-L-rhamno-pyranosyl-(1→2)-β-D-glucopyranoside]	oligosaccharide	+	-	-	+	(Yannai, 2003)
55	19.374	$C_{29}H_{46}O_4$	459.3496		$(M+H)^+$	459.3496 $(M+H)^+$, 332.3357 $((M+H-C_9H_{19})^+$	(3β, 5α, 9α, 22E, 24R)-3, 5, 9-trihydroxy-23-methyl ergosta-7, 22, diene-6-one	Steroid	+	+	+	-	(Yaoita, Amemiya, Ohnuma, Furumura, Masaki, Matsuki, et al., 1998)
56	19.866	$C_{33}H_{54}O_{11}$	671.3672	$(M+HCOO)^-$		671.3672 $(M+HCOO)^-$, 635.2622 $(M+HCOO-2H_2O)^-$, 617.2687 $(M+HCOO-3H_2O)^-$, 421.1605 $(M-H-Glu-C_3H_6)^-$	Ponasteroside A	Steroid saponin	+	-	-	-	(Hikino, Arihara, & Takemoto, 1969)

*Diox-Dioxolane substituent, Glu-Glucose, Ara-Arabinose, Glucu-Glucuronic acid, Rha-Rhamnose, Xyl-Xylose, Hex-Hexose, Pen- Pentose, UrA- Uronic acid

716

717 **Table 2.** ^{1}H (600MHz) and ^{13}C (150MHz) data of compound 1 & 2 in CD_3OD.

718

Position	1		2	
	δ_C, type	δ_H	δ_C, type	δ_H
1	39.6, CH_2	1.08 [a], 1.66 [a]	39.1, CH_2	1.07 [a], 1.67 [a]
2	26.3, CH_2	1.70 [a], 1.88 [a]	25.6, CH_2	1.92 [a], 1.74 [a]
3	86.4, CH	4.05 (dd, *J* =12.6, 4.8)	83.6, CH	3.86 [a]
4	53.9, C	-	56.1, C	-
5	52.9, CH	1.48 [a]	48.9, CH	1.31 [a]
6	21.7, CH_2	1.58 [a], 1.11 [a]	21.3, CH_2	0.88 [a], 1.49 [a]
7	33.5, CH_2	1.49 [a], 1.27 (m)	33.2, CH_2	1.22 [a], 1.48 [a]
8	40.9, C	-	40.9, C	-
9	49.1, CH	1.65 [a]	48.8, CH	1.68 [a]
10	37.4, C	-	37.0, C	-
11	24.5, CH_2	1.91 [a], 1.92 [a]	24.5, CH_2	1.91 [a], 1.91 [a]
12	123.5, CH	5.25 (t, *J* = 3.6)	123.5, CH	5.24 (s)
13	144.8, C	-	144.9, C	-
14	42.9, C	-	43.0, C	-
15	28.8, CH_2	1.78 [a],1.07 [a]	28.8, CH_2	1.76 [a],1.05 [a]
16	23.9, CH_2	1.71 [a], 2.04 (m)	23.6, CH_2	1.69 [a], 2.03 (m)
17	48.0, C	-	47.9, C	-
18	42.5, CH	2.85 (dd, *J* = 14.4, 4.8)	42.6, CH	2.84 (dd, *J* = 13.8, 4.8)
19	47.2, CH_2	1.15 [a], 1.71 [a]	47.1, CH_2	1.14 [a], 1.69 [a]
20	31.5, C	-	31.5, C	-
21	33.1, CH_2	1.62 [a], 1.72 [a]	33.0, CH_2	1.60 (m), 1.71 [a]
22	34.8, CH_2	1.22 (m), 1.39 (m)	34.8, CH_2	1.20 [a], 1.37 (m)
23	181.4, C	-	208.9, CH	9.39 (s)
24	12.2, CH_3	1.14 (s)	10.4, CH_3	1.09 (s)
25	16.2, CH_3	0.97 (s)	16.1, CH_3	0.98 (s)
26	17.5, CH_3	0.79 (s)	17.7, CH_3	0.79 (s)
27	26.2, CH_3	1.16 (s)	26.3, CH_3	1.16 (s)
28	178.1, C	-	177.9, C	-
29	33.4, CH_3	0.91 (s)	33.4, CH_3	0.90 [a]
30	23.9, CH_3	0.93 (s)	23.9, CH_3	0.92 [a]
	3-O-*β*-D-Glucuronic acid		**3-O-*β*-D-Glucuronic acid**	
1′	105.3, CH	4.38 (d, *J* = 7.8)	104.7, CH	4.29 (d, *J* = 7.8)
2′	74.3, CH	3.34 [a]	74.3, CH	3.31 [a]

3′	86.1, CH	3.51 [a]	86.4, CH	3.48 [a]
4′	71.5, CH	3.55 [a]	71.5, CH	3.53 [a]
5′	76.3, CH	3.76 (m)	76.4, CH	3.74 [a]
6′	172.6, C	-	172.9, C	-
	3'-O-*β*-D-xylose		**3'-O-*β*-D-xylose**	
1′′	105.7, CH	4.52 (d, *J* = 7.2)	105.7, CH	4.49 (d, *J* = 7.8)
2′′	75.2, CH	3.25 [a]	75.1, CH	3.25 [a]
3′′	77.5, CH	3.32 [a]	77.5, CH	3.32 [a]
4′′	70.9, CH	3.50 [a]	71.0, CH	3.34 [a]
5′′	67.0, CH_2	3.89 (dd. *J* = 11.4, 5.4Hz), 3.21 [a]	67.0, CH_2	3.88 [a], 3.21 [a]
	28-O-*β*-D-Glucose		**28-O-*β*- D-Glucose**	
1′′′	95.7, CH	5.38 (d, *J* = 8.4)	95.6, CH	5.37 (d, *J* = 7.8)
2′′′	73.9, CH	3.33 [a]	73.9, CH	3.31 [a]
3′′′	78.2, CH	3.41 [a]	78.2, CH	3.39 [a]
4′′′	71.1, CH	3.34 [a]	70.9, CH	3.49 [a]
5′′′	78.6, CH	3.34 [a]	78.6, CH	3.34 [a]
6′′′	62.4, CH_2	3.68 (m), 3.81 (m)	62.4, CH_2	3.67 [a], 3.79 [a]
δ in ppm, *J* in Hz, (m) multiplet, [a] overlapped signal				

719

720

721

722

723